Biomaterials 34 (2013) 3215–3222

Contents lists available at SciVerse ScienceDirect

Biomaterials

journal homepage: www.elsevier.com/locate/biomaterials

# The effect of forced growth of cells into 3D spheres using low attachment surfaces on the acquisition of stemness properties

Guannan Su [a,b,1], Yannan Zhao [a,1], Jianshu Wei [a,b,1], Jin Han [a], Lei Chen [a], Zhifeng Xiao [a], Bing Chen [a], Jianwu Dai [a,*]

[a] State Key Laboratory of Molecular Developmental Biology, Institute of Genetics and Developmental Biology, Chinese Academy of Sciences, Beijing 100101, China
[b] Graduate School, Chinese Academy of Sciences, Beijing 100190, China

ARTICLE INFO

*Article history:*
Received 3 December 2012
Accepted 7 January 2013
Available online 8 February 2013

*Keywords:*
Stemness
Reprogramming
3D sphere culture
Low attachment surface

ABSTRACT

Embryonic stem cells (ESCs) and neural progenitor cells form three-dimensional (3D) colonies or spheres *in vitro*, and 3D sphere is reported to help maintaining the stemness of stem cells, but the effect of 3D sphere formation on cell reprogramming remains unknown. Here we examined whether 3D sphere culture have any impact on the differentiated cells. We cultured bladder cancer cell RT4 and non-cancerous cell HEK293 on the low attachment dishes coated with soft agarose. When grown on this low attachment dish, cells spontaneously aggregated to form 3D spheres. Data showed that 3D sphere formation promoted the expression of reprogramming factors. Sphere formation of RT4 cells induced cancer stem cell characteristics including higher SP cell percentage, higher metastasis ability and higher tumorigenicity. HEK293 spheres showed upregulation of kidney progenitor cell markers and partially acquired characteristics of ESCs including upregulation of alkaline phosphatase activity, ES cell markers, three germ layer markers and tumorigenicity. The findings suggested that forced growth into 3D spheres by the low attachment surface could induce cells to acquire stemness properties.



## 1. Introduction

Proliferation while maintaining potency and differentiation capacity into specialized cell types endows stem cells with great promise for scientific research and therapeutic applications. Previous works demonstrated that pluripotent stem cells can be generated from somatic cells via overexpression of key transcription factors, creating a new method for cell reprogramming [1,2]. Since then, great efforts have been devoted to designing safer and more efficient methods for cell reprogramming, such as the utilization of proteins [3,4], RNAs [5], microRNAs [6] or defined chemicals [7,8]. Extrinsic cues have recently drawn great attention as accumulating evidences support that microenvironment can play a vital role in determining the properties of stem cells [9], suggesting that stem cell microenvironment might play an important role in cell reprogramming [10].

The microenvironment of cells is mainly composed of soluble growth factors, cell–matrix interactions and cell–cell interactions. Compared to conventional two-dimensional (2D) culture, cells cultured under three dimensional (3D) culture differ considerably in cell morphology, cell–cell contact and cell–matrix interactions [9,11–15]. Many 3D cell culture models have been established including the use of porous scaffolds, hydrogels or polymers. 3D self-organized cellular sphere is another typical 3D cell culture system taking advantage of the natural aggregation tendency of many cell types. Previous studies demonstrated sphere formation may be related to stemness since pluripotent cells tend to exhibit a sphere or colony morphology. For example, embryonic stem cells (ESCs) form colonies on feeder cells, and neural progenitor cells (NPCs) form typical neurospheres in suspension. Sphere-formation assays are also widely used to identify stem cells [16] and 3D sphere helps to maintain the stemness of stem cells. For instance, primary muscle stem cells can be maintained in culture as floating myospheres, retaining the potential to differentiate into muscle cells, adipocytes and osteogenic cells [17]. Cardiospheres recapitulate a niche-like microenvironment rich in stemness and cell–matrix interactions, rationalizing their enhanced functional potency for myocardial repair [18,19]. Spheroids of mesenchymal stem cells (MSCs) help to maintain the expression of stemness marker genes [20,21].

The close correlation between 3D sphere morphology and stemness promoted us to testify whether 3D sphere culture could induce non-stem cells to acquire stem cell properties. It is known

* Corresponding author. Institute of Genetics and Developmental Biology, Chinese Academy of Sciences, 3 Nanyitiao, Zhongguancun, Beijing 100190, China. Tel./fax: +86 (0)10 82614426.
*E-mail address:* jwdai@genetics.ac.cn (J. Dai).
[1] These authors contributed equally to this work.

0142-9612/$ – see front matter © 2013 Elsevier Ltd. All rights reserved.
http://dx.doi.org/10.1016/j.biomaterials.2013.01.044

that cellular spheroids can be commonly obtained through three approaches. The first one is hanging drop method that spheres are grown in droplets placed on an inverted plate [22]. The second is gyratory rotation technique that trypsinized cells are cultured in a stirred flask to prevent them from adhering to the substrate [23]. The third one is low-attachment cultivation of cells on hydrophobic surface [24]. In this work, we prepared low attachment surface by coating soft agarose on cell culture dish, and performed 3D sphere culture of human urinary bladder papilloma cell line RT4 and human embryonic kidney epithelial cell line HEK293, representing cancer and non-cancerous cells respectively. Compared with conventional 2D culture, 3D sphere culture promoted the expression of reprogramming factors. Sphere formation of RT4 cells induced cancer stem cells characteristics including higher SP cell percentage, higher metastasis ability and higher tumorigenicity. HEK293 spheres showed upregulation of kidney progenitor cell markers and partially acquired characteristics of ESCs including upregulation of alkaline phosphatase activity, ES cell markers, three germ layer markers and tumorigenicity.

## 2. Materials and methods

### 2.1. Preparation of low attachment dish

For the preparation of 2× DMEM medium, 13.4 g DMEM high glucose (Powder) (GIBCO) and 3.7 g sodium bicarbonate were dissolved in 500 mL deionized water and sterilized by 0.22 micron filter. 2× DMEM medium was pre-warmed to 37 °C. 1% agarose solution was made with agarose G-10 (BIOWEST) and deionized water and heated until boiling in microwave. Equal volume of pre-warmed 2× DMEM medium and 1% agarose solution was mixed and coated on cell culture dish. When temperature declined, agarose and DMEM mixture will form a layer of 0.5% gel with a thickness of 4 mm.

### 2.2. Cell culture

HEK293 cell line was purchased from Peking Union cell center (ATCC source) and RT4 cell line was presented by Professor Ying Jin, Shanghai Jiao Tong University.

RT4 and HEK293 cells were cultured in McCOY'5A(HYCLONE) and DMEM(HYCLONE) medium respectively, both supplemented with 10% FBS (GIBCO), 1 mM L-glutamin (Sigma), 1 mM sodium pyruvate (GIBCO), 0.1 mM NEAA (GIBCO) and 50 units of penicillin/streptomycin (HYCLONE). The cells were cultured at 37 °C in 5% $CO_2$, and the medium was changed every 2 days. When cells have reached 90% confluence, they were trypsinized with 0.25% trypsin (Amresco) and passaged at a ratio of 1:3. For 3D culture, $3 \times 10^6$ RT4 or HEK293 cells were transferred to a 60 mm low attachment dish. These cells were cultured at 37 °C with 5% $CO_2$. Medium was changed every other day.

### 2.3. Alkaline phosphatase (AP) staining

For AP staining, cells were fixed with 60% acetone (diluted with 1.5M sodium citrate solution) for 1 min. The fixed cells were then washed with PBS for 1 min and then stained with BCIP/NBT solution (Sigma). For BCIP/NBT solution, 330 ul NBT solution and 33 ul BCIP solution were diluted with 10 mL AP working solution (0.1M Tris-base, 100 mM NaCl, 5 mM $MgCl_2$, PH 9.5). The staining process was terminated when purple stainings arised.

### 2.4. Quantitative RT-PCR

Total RNAs of monolayer and sphere cells were extracted with Trizol reagent (Invitrogen) according to manufacturer's instructions. Total RNA concentration was determined by optical density at 260 nm (OD260) using a spectrophotometer (Amersham Biosciences). After removing residual DNA with Dnase I (Invitrogen), equal amounts of RNA (1 μg) were added to reverse transcriptase reaction mix (SuperScript III First-Strand Synthesis System, Invitrogen) with oligo-dT primers (Invitrogen). Power SYBR Green RT-PCR Kit (Applied Biosystems) was utilized to perform Q-PCR using the Bio-RAD CFX96 Real-Time system (Bio-RAD). The expression level was analyzed and normalized to GAPDH for each cDNA sample. Fold change of gene expression was calculated using the 2-ΔΔCT method. Primer sequences were available in Table S1.

### 2.5. Nude mice tumor formation assay

All experiments on animals were subjected to Chinese Ministry of Public Health (CMPH) Guide. Cells with or without trypsinization, were suspended in DMEM medium mixed with an equal volume of ECM (Sigma) to a final volume of 200 μl. Cells were injected subcutaneously by 27-gauge needles into the back flanks of 4–5 week old nude mice (8 BALB/c-nu). The mice were monitored twice a week for signs of tumor growth for 2 months. Tumors were fixed in 4% paraformaldehyde and sectioned to 5 μm thickness for hematoxylin-eosin (H&E) staining.

### 2.6. Western blot

Cells were washed with PBS and lysed in RIPA (Sigma) buffer with Complete Protease Inhibitor Cocktail (Roche) for 30 min on ice to prepare the whole cell lysates. Protein concentrations were measured using Protein Assay against BCA standards (PIERCE). Equivalent quantity of protein lysates were electrophoresed in 12% SDS-ploy acrylamide gel, and transferred to a polyvinylidene difluoride membrane (Amershame). The membrane was blocked in TBS containing 10% nonfat milk and 0.05% tween-20 for 2 h at the room temperature. Primary antibodies were incubated for 2 h at the room temperature, and primary antibodies included: NANOG (1:5000, Abcam), SOX2 (1:200, Invitrogen) and beta-Actin (1:500, Santa Cruz). The HRP labeled secondary antibody was incubated for 2 h at the room temperature. Secondary antibodies conjugated with HRP included: Goat-Anti Mouse IgG (1:10,000, SouthernBiotech) and Goat-Anti Rabbit IgG (1:3000, Thermo Scientific).

### 2.7. Side population analysis using flow cytometry

Monolayer and sphere RT4 cells were trypsinized with accutase (Sigma) and then cells were suspended at $1 \times 10^6$ cells/mL in DMEM medium supplemented with 2% FBS. These cells were then incubated at 37 °C for 90 min in darkness with 5 μg/mL Hoechst 33342 (Sigma), either alone or in the presence of 50 μg/mL verapamil (Sigma). At the end of incubation, cells were spun down in the cold and resuspended in ice-cold PBS with 2% FBS. After washing with PBS, the cells were treated with 2 μg/mL propidium iodide to exclude dead cells. SP analysis was done using a FACSVantage SE (BD Biosciences).

### 2.8. Cell migration assay

For measurements of cell migration, RT4 cells under monolayer and 3D culture conditions were pre-treated with 24 h serum hungry. Then the monolayer and sphere cells were trypsinized by 0.25% trypsin/EDTA and resuspended in McCOY'5A media containing no FBS as a density of $5 \times 10^5$ cells/mL. 200 μl cells in suspension were plated on the top chamber of 24-well transwell containing 8 μm pores (Corning). 600 μl medium with 10% FBS was added to the bottom chamber. Cells were allowed to migrate in response to FBS. After 24 h, migrated cells on the bottom were stained with 0.1% crystal violet. The number of stained cells on the bottom surface was counted under the microscope and four independent fields were counted for each Transwell.

### 2.9. Transient transfections and luciferase reporter assays

For DNA transfections, HEK293 ($8 \times 10^4$) cells were seeded per well of 24-well plates 16 h prior to transfection. The monolayer cells were then transfected with 800 ng DNA plasmids using Lipofectamine 2000 (Invitrogen) according to the protocol supplied. Media was replaced at 6 h post-transfection.

Oct4-Luc vector was constructed by inserting 6W enhancer into PGL3 vector with tk promoter. Nanog-Luc vector was kindly provided by Pro. Duanqing Pei. Sox2/Oct4-Luc vector was kindly provided by Pro. Lisa Dailey. Reporter plasmids were extracted using the Plasmid Mini Kit I (OMEGA) with standard protocol. Transfection was performed according to the manufacturer's instruction. Being cultured for 24 h after transfection, cells were trypsinized and subjected to 2D and 3D cultures respectively. Luciferase assay was carried out according to the standard protocol (Promega).

### 2.10. Bisulfate sequencing

Genomic DNA was extracted from monolayer and sphere cells using QIAamp DNA Mini Kit (Qiagen). Bisulfite treatment was performed using Epi-Tect Bisulfite kit (Qiagen) according to the manufacturer's recommendations. The transcription regulatory regions of *OCT4*, *NANOG* and *SOX2* were amplified by PCR (Hotstar HiFidelity DNA polymerase, Qiagen). Primer sequences used for PCR amplification were provided in Table S1. The PCR products were subcloned into pMD18-T vector (TaKaRa) and individual clones were then sequenced. Clones were only accepted with more than 90% cytosine conversion. BiQ Analyzer software (Max Planck Society) was used for the quality check and methylation analysis. At least 20 replicates were analyzed for each sequence.

### 2.11. Statistical analysis

The statistical significance (*P* values) in mean values of two-sample comparison was determined with Students' *t*-test. A value of $P < 0.05$ was considered statistically significant (*) and a value of $P < 0.01$ was considered extremely significant (**). Values shown on graphs represent the means ± s.d.

## 3. Results

### 3.1. Reprogramming transcription factor expression in 3D RT4 spheres

To create a low attachment surface, we coated cell culture dish with a 4 mm layer of 0.5% agarose, prepared by mixing 1% agarose and 2× DMEM medium (Fig. 1A). Covered with PBS, the low attachment dish can be stored for months at 4 °C. When trypsinized cells were cultured on low attachment dish, they formed 3D free-floating spheres within 24 h. Arrow indicates cell spheres suspended on low-attachment dish (Fig. 1B).

Utilizing this method, we performed 3D sphere culture on human urinary bladder papilloma cell line RT4 cells. Previous studies demonstrated suspension culture of cancer cells with growth factors in serum-free or low-serum medium being a method to enrich cancer stem cells. We here attempted to minimize the influence of culture medium and just focused on the effect of 3D sphere culture. Instead of using serum-free medium supplemented with growth factors, we used complete growth medium with 10% fetal bovine serum. As shown in Fig. 1C, cells under conventional monolayer culture adhered to cell culture dish and demonstrated epithelial morphology. In contrast, cells cultured on low attachment dish were detached from the plate and formed floating 3D spheres. The spheres maintained stable morphology even after several days. OCT4, NANOG and SOX2 are core transcription factors for embryonic stem (ES) cells, which are important for maintaining the pluripotent and self-renewal capacities of stem cells. OCT4, SOX2, NANOG, LIN28 or OCT4, SOX2, c-MYC, KLF4 have been used to reprogram human somatic cells into induced pluripotent stem cells (iPSCs). By Q-PCR, we found *OCT4*, *NANOG*, *SOX2*, *KLF4* and *c-MYC* were upregulated in sphere culture compared to monolayer culture (Fig. 1D). We also found the protein levels of NANOG and SOX2 were significantly upregulated in RT4 spheres by western blot (Fig. 1E).

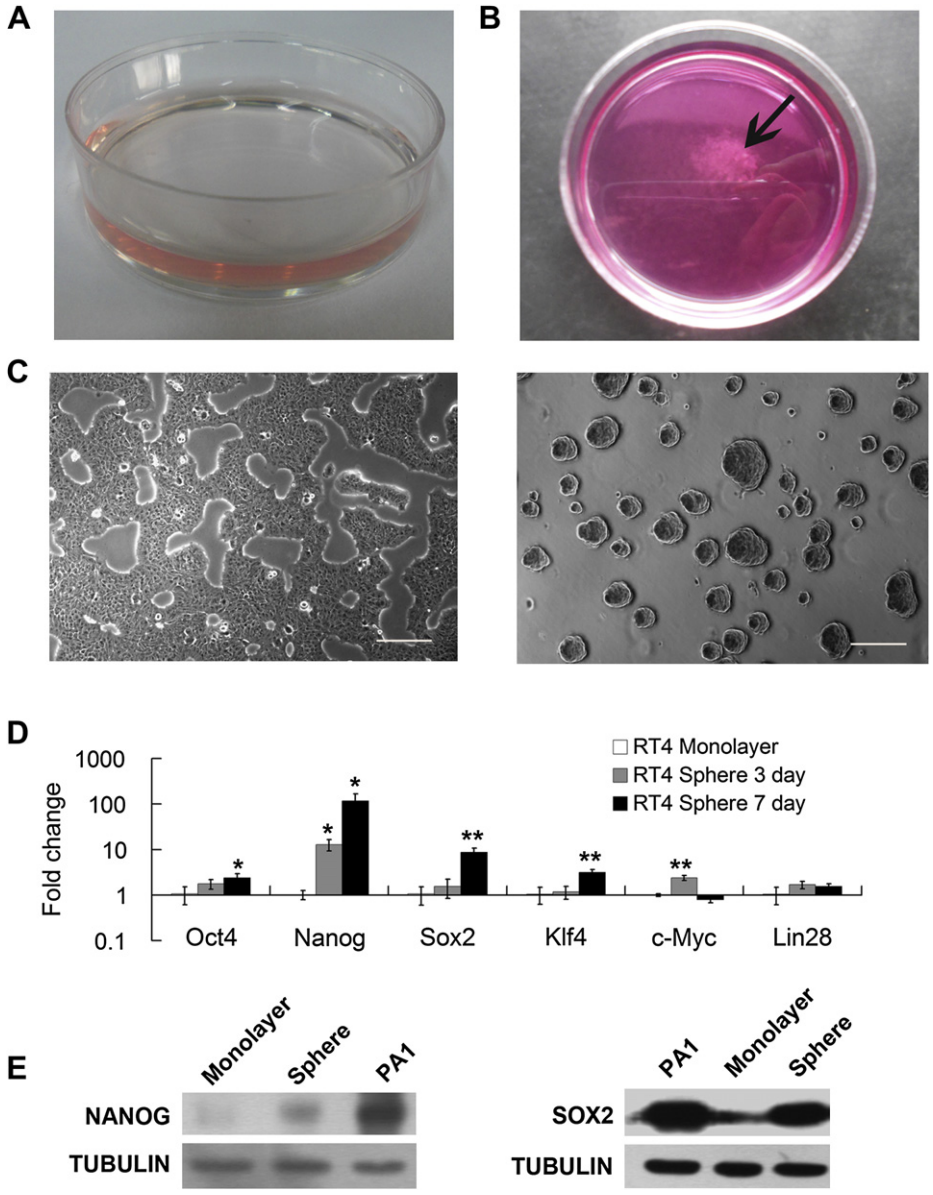


**Fig. 1.** Upregulation of reprogramming transcription factors in 3D RT4 spheres. A. Agarose coated low attachment dish. B. Cells grown on low attachment dish acquired sphere morphology. Arrow indicated 3D cell spheres. C. Phase-contrast images of RT4 cells in monolayer (left) and sphere culture (right). Scale bars = 200 μm. D. Q-PCR analysis for *OCT4, NANOG and SOX2* of RT4 cells in monolayer and sphere culture ($n = 3$). *GAPDH* was used to normalize the quantitative real time results. E. Western blotting for NANOG and SOX2 expression of RT4 cells in monolayer and 7-day-sphere culture. Teratoma cell line PA-1 was used as positive control.

### 3.2. Cancer stem cell characteristics of 3D RT4 spheres

Cancer stem cell characteristics of 3D RT4 spheres including "side population" (SP) percentage, metastasis ability, and tumorigenicity were analyzed. SP discrimination assay, a method to detect stem cell percentage using dye efflux properties of stem cells, is often used in cancer stem cell evaluation [25]. The percentage of SP cells in sphere culture was 0.83 ± 0.32%, compared to 0.37 ± 0.12% in monolayer culture (Fig. 2A). Metastasis of cancer cell is also correlated with the stem cell characteristics. Low differentiation level of cancer cells is correlated with greater risk of metastasis [26]. We detected the metastasis ability of RT4 cell by transwell assay, and the

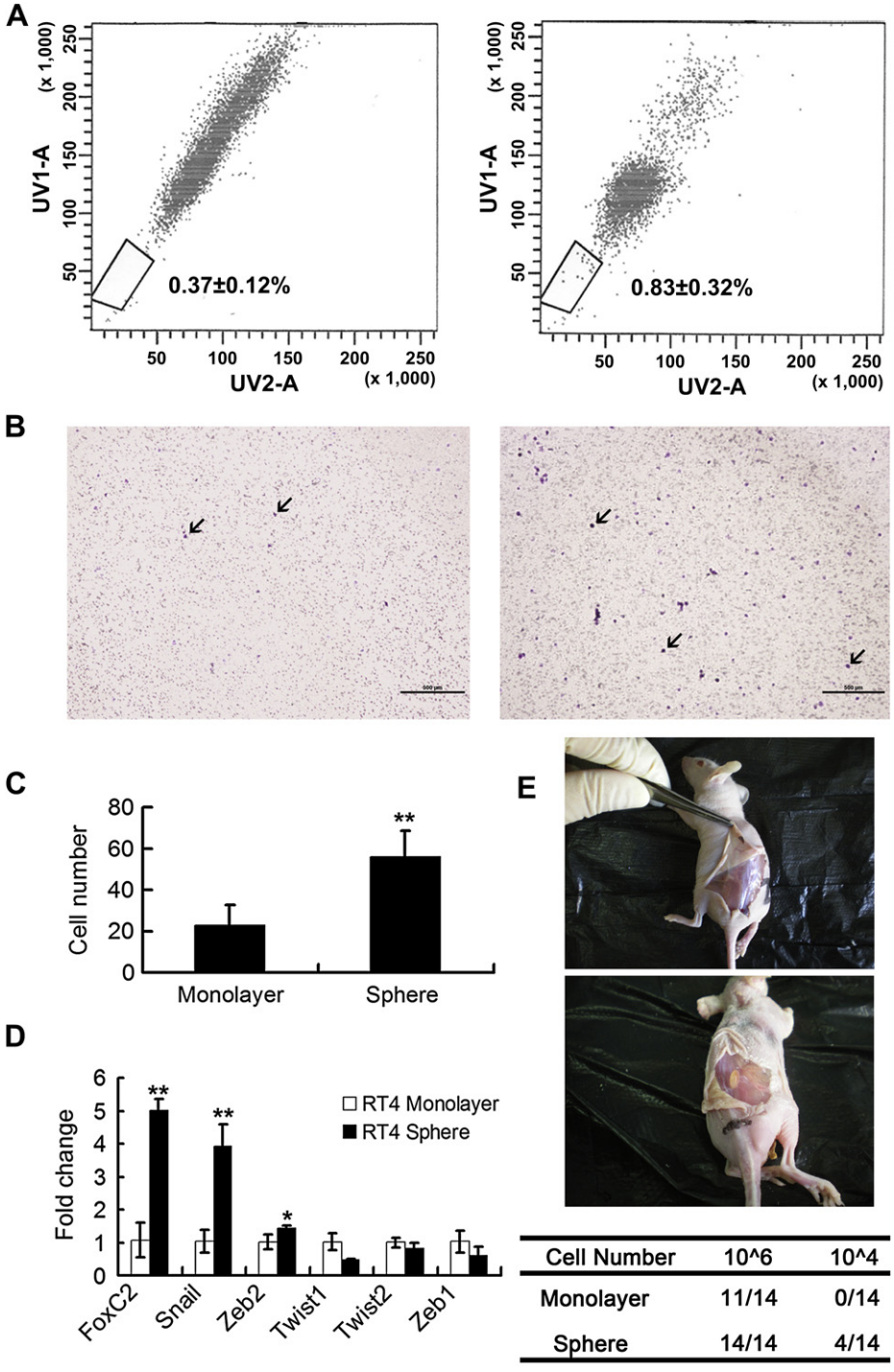


| Cell Number | 10^6 | 10^4 |
|---|---|---|
| Monolayer | 11/14 | 0/14 |
| Sphere | 14/14 | 4/14 |

**Fig. 2.** 3D sphere formation of RT4 cells upregulated characteristics of cancer stem cell. A. Side population (SP) percentage of RT4 cells in monolayer (left) and 7-day-sphere culture (right) ($n = 3$). B, C. Transwell experiment for RT4 cell metastatic ability. Representative photomicrographs of transwell results for RT4 cell in monolayer (left) and 7-day-sphere culture (right). Arrow heads indicate crystal violet stained migrated cells (B). Quantitative analysis of migrated cells in monolayer and 7-day-sphere culture. 4 Stochastic fields were counted for each experimental group (C). D. Q-PCR analysis for genes related to epithelial mesenchymal transition (EMT) of RT4 cells in monolayer and 7-day-sphere culture ($n = 3$). E. Nude mice tumor formation assay of RT4 cells. $1 \times 10^6$ or $1 \times 10^4$ RT4 cells were injected subcutaneously into the back of nude mice. Tumors failed to form when $1 \times 10^4$ RT4 monolayer cells were injected (up). Tumors formed when $1 \times 10^4$ RT4 sphere derived cells were injected (bottom). The table is a summary for tumor formation assay. Monolayer indicates trypsinized RT4 cells in monolayer culture; sphere indicates trypsinized RT4 sphere cells.

results indicated sphere culture promoted cell metastasis ability (Fig. 2B, C). Epithelial mesenchymal transition (EMT) is a key development program for cancer invasion and cancer stem cell property [27]. Gene expression associated with EMT was examined by Q-PCR. The results demonstrated *FOXC2*, *SNAIL* and *ZEB2* were upregulated in RT4 spheres compared to the monolayer (Fig. 2D). We also performed *in vivo* nude mice tumor formation assay. As shown in Fig. 2E and $1 \times 10^6$ monolayer RT4 cells formed tumors in 11 out of 14 mice, while $1 \times 10^6$ sphere derived RT4 cells formed tumors in 14 out of 14 mice. Furthermore, $1 \times 10^4$ monolayer RT4 cells failed to form any tumors, while $1 \times 10^4$ sphere derived cells formed tumors in 4 out of 14 mice. The data indicated that 3D sphere culture of RT4 tumor cells promoted cancer stem cell properties.

### 3.3. Reprogramming transcription factor expression in 3D HEK293 spheres

HEK293 is a non-cancerous cell line originally derived from human embryonic kidney cells. HEK293 cells adhered to the cell culture dish and showed monolayer epithelial morphology, while cultured on the low attachment plate HEK293 formed floating 3D spheres (Fig. 3A). Q-PCR analyses of reprogramming factors showed that *OCT4*, *NANOG*, *SOX2*, *KLF4* and *LIN28* were all upregulated in sphere culture at 5 and 10 days compared to monolayer culture (Fig. 3B). Western blotting analyses also showed that the protein levels of NANOG and SOX2 in sphere culture group were higher compared to the monolayer group (Fig. 3C). Luciferase reporter constructs of the binding sequences of OCT4, NANOG or SOX2/OCT4 were introduced into HEK293 cells to detect the transcription activity of these transcriptional factors. We found that OCT4, NANOG and SOX2/OCT4 proteins in 3D cells had higher transcription activities (Fig. 3D). Similarly, bisulfite genomic sequencing analyses evaluating the methylation status of cytosine guanine dinucleotides (CpG) in the transcriptional regulatory regions of *OCT4*, *NANOG* and *SOX2* revealed that the methylation status in HEK293 spheres was lower than those in monolayer HEK293 cells (Fig. 3E), indicating these genes were more transcriptionally activated than monolayer cells.

### 3.4. Embryonic stem cell phenotype of 3D HEK293 spheres

Alkaline phosphatase activity is an early event during the induction process of iPS cells. We found AP staining was positive in

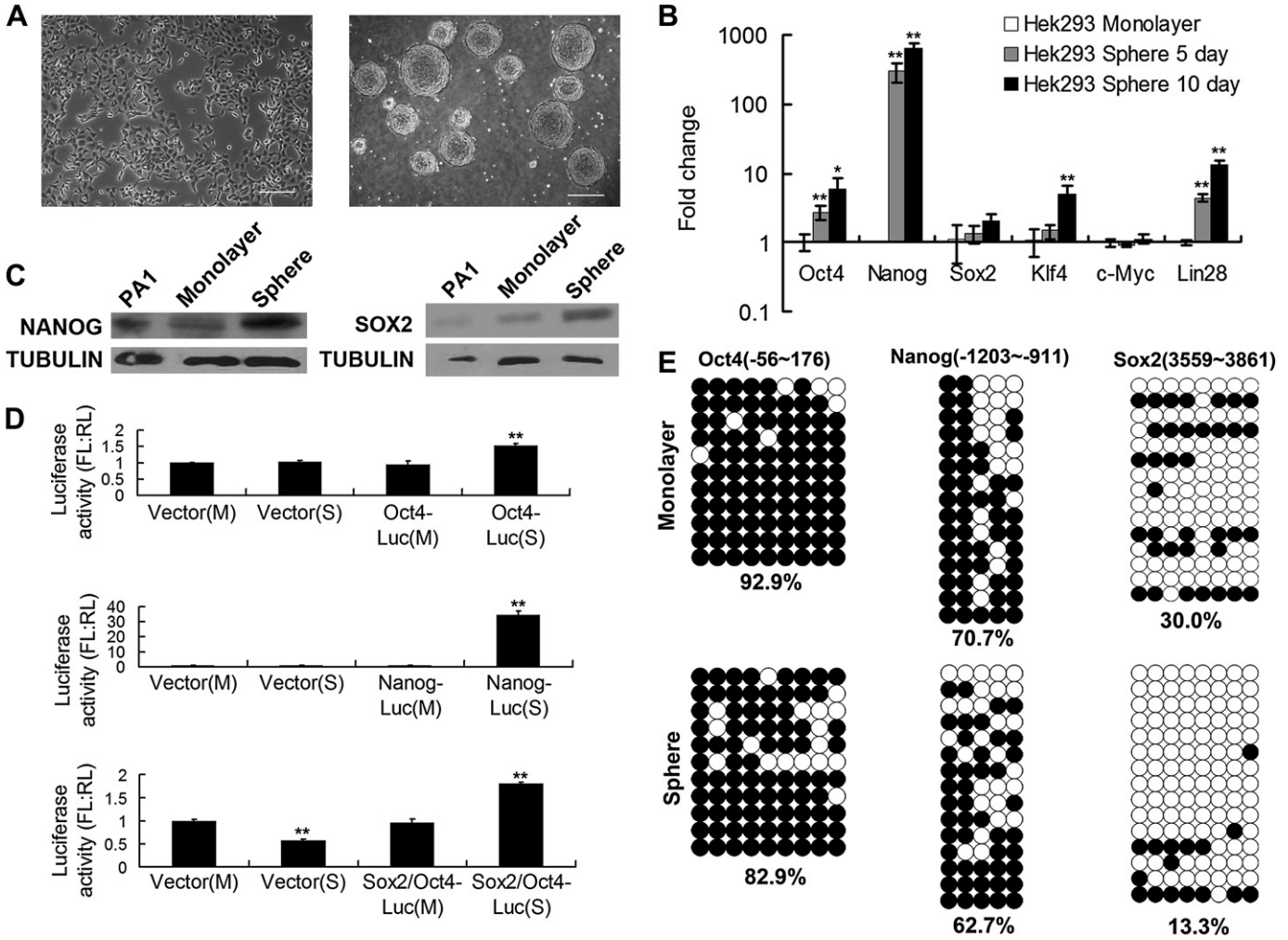


**Fig. 3.** Upregulation of reprogramming transcription factors in 3D HEK293 spheres. A. Phase-contrast images of HEK293 cells in monolayer (left) and sphere culture (right). Scale bars = 200 μm. B. Q-PCR analysis for *OCT4*, *NANOG* and *SOX2* of HEK293 cells in monolayer and sphere culture ($n = 3$). C. Western blotting for NANOG and SOX2 expression of HEK293 cells in monolayer and 10-day-sphere culture. D. Luciferase assay indicating OCT4, NANOG and OCT4/SOX2 transcriptional activities in monolayer and sphere HEK293 cells. Vector indicates control luciferase reporter. Oct4-Luc, Nanog-Luc and Sox2/Oct4-Luc represent luciferase reporter construct with the transcription binding site of OCT4, NANOG and SOX2/OCT4 respectively. (M) indicates monolayer cells and (S) indicates 10-day-sphere cells ($n = 3$). E. Bisulfite genomic sequencing of the transcriptional regulatory regions of *OCT4*, *NANOG* and *SOX2* of HEK293 cells in monolayer and 10-day-sphere culture. Monolayer methylation status is shown on the top in each panel. 10-day-sphere methylation status is shown on the bottom in each panel. The transcriptional starting site is designated as +1. Open circles indicate unmethylated CpGs, while closed circles indicate methylated CpGs.

HEK293 sphere cells but negative in monolayer cells (Fig. 4A). By Q-PCR analyses, mRNA expression of several undifferentiated ES cell markers was also tested. The data showed that *REX1*, *TDGF1*, *LEFTB*, *EBAF*, *GRB7*, *PODXL* and *FGF4* were upregulated in HEK293 3D cells (Fig. 4B). Moreover, endoderm markers (*FOXA2*, *AFP*, *SOX17* and *PDX-1*), mesoderm markers (*BRANCHYURY* and *MSX1*) and ectoderm markers (*NESTIN*, *OTX2* and *TP63*) were all upregulated in spheres (Fig. 4C). As kidney-derived HEK293 cells are derived from mesoderm, the up-regulation of endoderm and ectoderm markers also indicated cell reprogramming occurred. ESCs could form teratomas when injected into nude mice, therefore the tumorigenicity of HEK293 spheres was examined *in vivo*. As shown in Fig. 4D, $3 \times 10^6$ HEK293 monolayer cells failed to form any tumors, while $3 \times 10^6$ HEK293 spheres formed tumors in 3 out of 7 mice and trypsinized sphere cells formed tumor in 1 out of 7 mice. Although from HE staining of tumor sections formed by sphere cells, no definite structures of endoderm, mesoderm or ectoderm were detected, the tumorigenic properties suggesting the dedifferentiation occurred in HEK293 spheres.

### 3.5. Kidney progenitor characteristics of 3D HEK293 spheres

As HEK293 cells are derived from kidney tissues, we detected kidney progenitor phenotype of HEK293 spheres. As illustrated in Fig. 5A, metanephric mesenchyme, where kidney progenitor cells reside, is the direct precursor tissue of adult kidney, which further differentiates into nephrons. We found renal progenitor cell markers *PAX2*, *WT1*, *INTEGRIN a8*, *SALL1*, *LIM1*, *NCAM1*, *SIX2*, *FRIZZLED 2*, *FRIZZLED 7*, *ACVR2b* and *NTRK2* were upregulated in HEK293 spheres (Fig. 5B). We also testified whether kidney progenitor cells in HEK293 spheres possess the potential of differentiation into nephrons. Terminally differentiated nephron markers of glomeruli, proximal tubule, Henle's loop and distal tubule were examined by Q-PCR. Glomeruli markers (*NPHS1*, *ACTN4*, *CD2AP*, *CDH3*, *PDPN* and *PODXL*), proximal tubule markers (*AQP1*, *CLCN5*, *CUBN*, *LRP2* and *SLC5A1*), Henle's loop markers (*UMOD* and *PKD2*) and distal tubule (*SCNN1a* and *PKD1*) of HEK293 spheres were all upregulated significantly after they were cultured for 5 and 10 days in 3D spheres (Fig. 5C–F). The data suggested that the sphere culture could promote kidney tissue specific dedifferentiation that possessing differentiation tendency into mature renal units.

## 4. Discussion

Here we show through 3D sphere culture on the low attachment dishes, RT4 and HEK293 cells were reprogrammed and acquired stemness properties, without involvement of any exogenous genes, RNAs or proteins. The exact reprogramming mechanisms remain elusive, but the close relationship between stem cell niche and cell fate decisions has been documented. Stem cell microenvironment influences stem cells in making decision to remain a quiescent state, to undergo self-renewal or to exit the niche [28] and mediates dedifferentiation and reprogramming of ectopic or more differentiated cells to the corresponding stem cell phenotype [29–31]. We speculate 3D sphere cultures may provide a microenvironment to promote cell dedifferentiation or reprogramming. First, sphere culture may form inner hypoxia compared to monolayer culture [32], as reported by many studies indicating hypoxic conditions help maintaining the pluripotency of stem cells [33–36]. Secondly, cell shape is a potent regulator of cell growth, physiology, embryonic development and stem cell differentiation [37–40], which might be attributed to the re-organization of cytoskeleton [41]. Cells within 3D sphere cultures can form different cell shapes [42]. We observed sphere derived adherent cells present various morphologies compared to 2D culture. Thirdly, extracellular matrix can exert exquisite control over stem cell fate decisions, mediated by several classes of receptors, the most extensively studied being integrins [43–46]. 3D sphere culture may form distinct extracellular matrix and establish new cell–matrix interactions to influence cell fate. In addition, 3D sphere culture presented several other differences from monolayer culture, including slower diffusive transport of soluble factors, concentration gradients of signaling factors, mechanical inputs and different spatial presentation of regulatory cues from all directions [47].

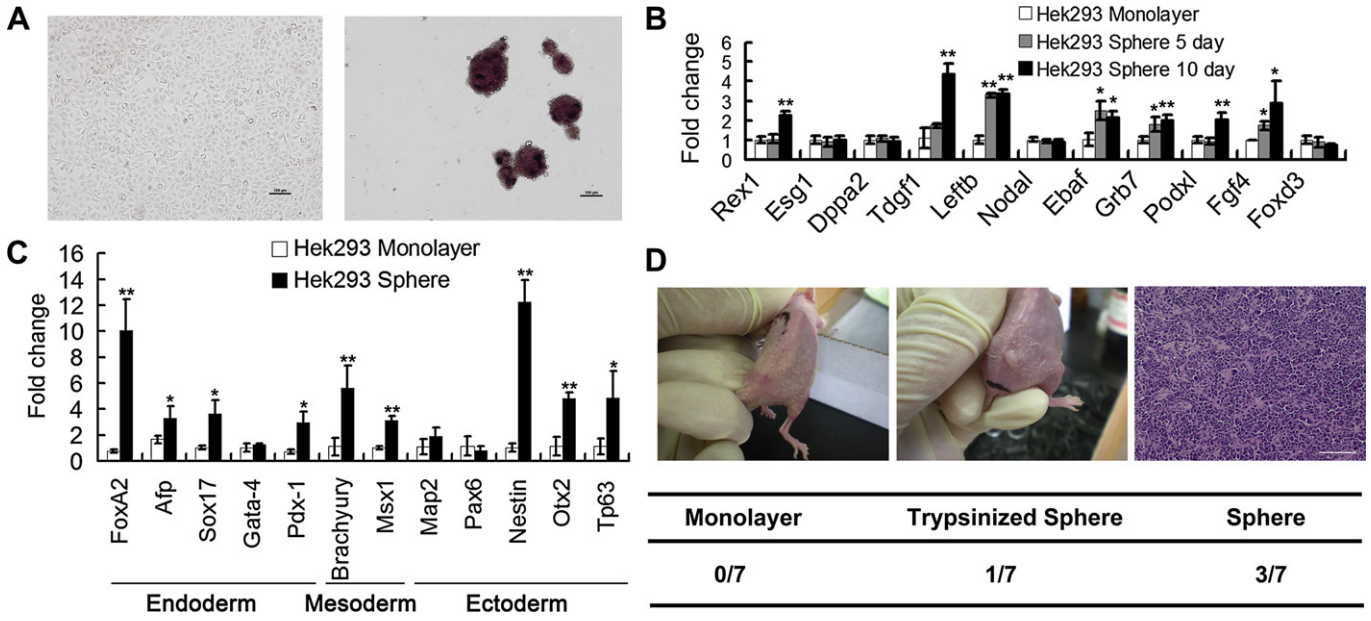


| Monolayer | Trypsinized Sphere | Sphere |
|---|---|---|
| 0/7 | 1/7 | 3/7 |

**Fig. 4.** HEK293 cells in 3D sphere partially gained embryonic stem cell phenotype. A. Alkaline phosphatase staining for HEK293 cells in monolayer (left) and 10-day-sphere culture (right). B. Q-PCR analysis for ESC marker genes of HEK293 cells in monolayer and sphere culture ($n = 3$). C. Q-PCR analysis for marker genes of endoderm, mesoderm and ectoderm of HEK293 cells in monolayer and 10-day-sphere culture ($n = 3$). D. Nude mice tumor formation assay. Monolayer HEK293 cells failed to form tumors (left in Fig. D). 3D HEK293 cells formed tumors (middle in Fig. D). HE staining of tumor section formed by HEK293 sphere cells (right in Fig. D). The table is a summary for tumor formation assay. Monolayer indicates trypsinized HEK293 cells in monolayer culture; trypsinized sphere indicates trypsinized HEK293 cell spheres; sphere indicates non-trypsinized HEK293 spheres.

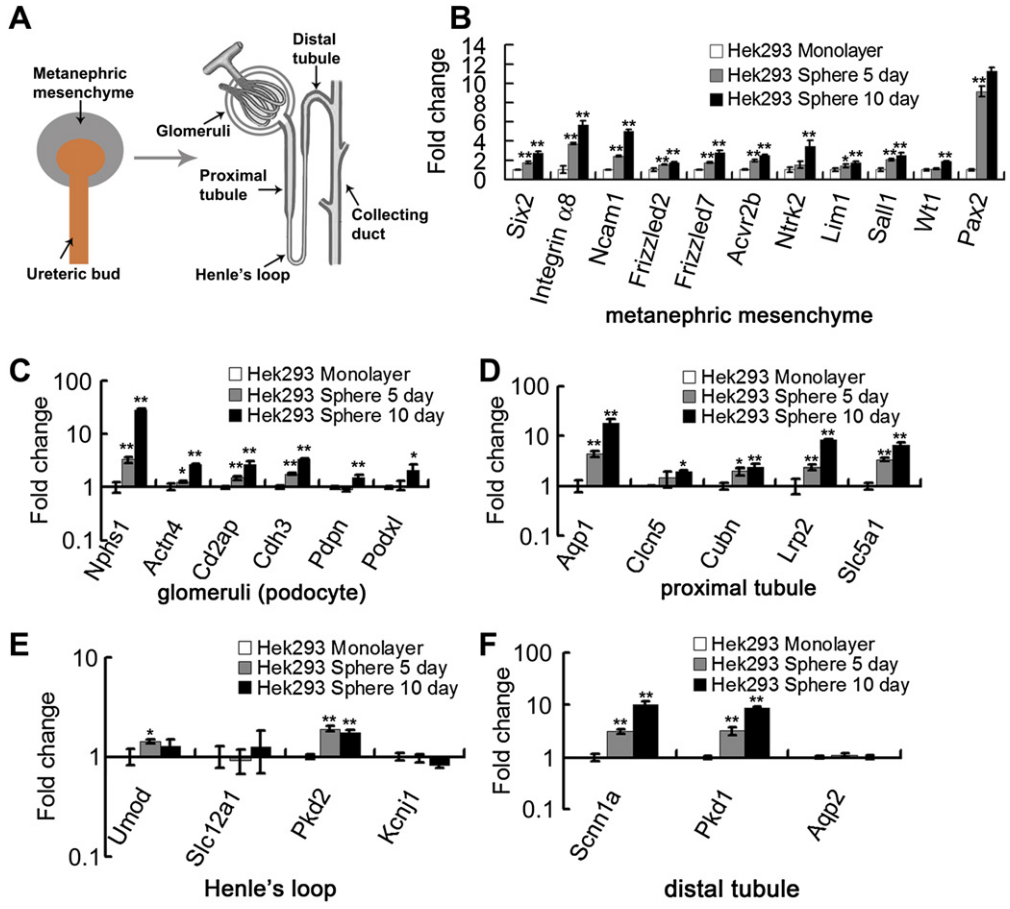


**Fig. 5.** Upregulation of kidney progenitor markers in HEK293 3D cells. A. Sketch map of renal unit. B–F. Q-PCR analysis for genes expressed in metanephric mesenchyme (B), glomeruli (podocyte) (C), proximal tubule (D), Henle's loop (E) and distal tubule(F) of HEK293 cells in monolayer, 5-day-sphere culture and 10-day-sphere culture.

Through 3D sphere culture, RT4 and HEK293 cells acquired stemness to various degrees. It might be attributed to the different cell characteristics and the diverse microenvironments formed in RT4 and HEK293 spheres. Cancer stem cells have the exclusive ability to self-renew and to differentiate into the heterogeneous lineages of cancer cells that comprise the tumor. We found 3D sphere culture of RT4 cells promoted cancer stem cell phenotypes. It is similar with previous study that mutation of RB1 gene promoted mouse fibroblasts to form spheres and to undergo reprogramming to cancer stem cells [42]. As HEK293 cells are derived from embryonic kidney tissues, HEK293 spheres presented phenotypes of ESCs and kidney progenitor cells. Osafune et al. reported single renal progenitor cells derived from metanephric mesenchyme tend to form colonies, and these colonies maintain differentiation capabilities into glomeruli and renal tubules [48]. So kidney specific reprogramming in 3D HEK293 spheres might be related with the features of kidney progenitors. There are still questions waiting to be answered such as the cells were not fully reprogrammed, and the decreased methylation in *OCT4*, *NANOG* and *SOX2* transcription regulatory regions may not be sufficient to activate the expression of these genes to comparable levels of ESCs. High-throughput screening of chemicals such as DNA methyltransferase and histone deacetylase inhibitors [49] to obtain fully reprogrammed cells might be attempted in future. Further investigations of the effects of 3D sphere culture on fibroblasts remain to be done to find a safer and more practical technique to reprogram patient-derived somatic cells.

## 5. Conclusion

By utilizing non-adherent substrates, 3D spheres of RT4 and HEK293 cells were obtained. The results demonstrated that these cells were reprogrammed and acquired stemness to various degrees through this physical method, without using any exogenous genes, RNAs or proteins. 3D sphere culture could provide better understanding of the cell stemness regulation and shed light on finding a safer and more practical technique to reprogram cells with physical approaches.

## Acknowledgments

We thank Pro. Ying Jin at the Shanghai Stem Cell Institute of Shanghai Jiao Tong University School of Medicine for providing the RT4 cell line. We thank Pro. Duanqing Pei at the Guangzhou institutes of Biomedicine and Health, Chinese Academy of Sciences for providing Nanog-Luc vector. This work was supported by grants from the Ministry of Science and Technology of China (2011CB965001) and the "Strategic Priority Research Program" of the Chinese Academy of Sciences (Grant No. XDA01030401).

## Appendix A. Supplementary data

Supplementary data related to this article can be found at http://dx.doi.org/10.1016/j.biomaterials.2013.01.044.

## References


[1] Takahashi K, Yamanaka S. Induction of pluripotent stem cells from mouse embryonic and adult fibroblast cultures by defined factors. Cell 2006;126:663–76.

[2] Yu J, Vodyanik MA, Smuga-Otto K, Antosiewicz-Bourget J, Frane JL, Tian S, et al. Induced pluripotent stem cell lines derived from human somatic cells. Science 2007;318:1917–20.

[3] Kim D, Kim CH, Moon JI, Chung YG, Chang MY, Han BS, et al. Generation of human induced pluripotent stem cells by direct delivery of reprogramming proteins. Cell Stem Cell 2009;4:472–6.

[4] Zhou H, Wu S, Joo JY, Zhu S, Han DW, Lin T, et al. Generation of induced pluripotent stem cells using recombinant proteins. Cell Stem Cell 2009;4:381–4.

[5] Warren L, Manos PD, Ahfeldt T, Loh YH, Li H, Lau F, et al. Highly efficient reprogramming to pluripotency and directed differentiation of human cells with synthetic modified mRNA. Cell Stem Cell.7:618–30.

[6] Anokye-Danso F, Trivedi CM, Juhr D, Gupta M, Cui Z, Tian Y, et al. Highly efficient miRNA-mediated reprogramming of mouse and human somatic cells to pluripotency. Cell Stem Cell.8:376–88.

[7] Shi Y, Do JT, Desponts C, Hahm HS, Scholer HR, Ding S. A combined chemical and genetic approach for the generation of induced pluripotent stem cells. Cell Stem Cell 2008;2:525–8.

[8] Zhu S, Li W, Zhou H, Wei W, Ambasudhan R, Lin T, et al. Reprogramming of human primary somatic cells by OCT4 and chemical compounds. Cell Stem Cell.7:651–5.

[9] Nur EKA, Ahmed I, Kamal J, Schindler M, Meiners S. Three-dimensional nanofibrillar surfaces promote self-renewal in mouse embryonic stem cells. Stem Cells 2006;24:426–33.

[10] Eshghi S, Schaffer DV. Engineering microenvironments to control stem cell fate and function. In: Bhatia Sangeeta, Polak Julia, editors. StemBook. Cambridge (MA): Harvard Stem Cell Institute; 2008. http://dx.doi.org/10.3824/stembook .1.5.1.

[11] Yamada KM, Cukierman E. Modeling tissue morphogenesis and cancer in 3D. Cell 2007;130:601–10.

[12] Birgersdotter A, Sandberg R, Ernberg I. Gene expression perturbation in vitro–a growing case for three-dimensional (3D) culture systems. Semin Cancer Biol 2005;15:405–12.

[13] Cukierman E, Pankov R, Stevens DR, Yamada KM. Taking cell-matrix adhesions to the third dimension. Science 2001;294:1708–12.

[14] Griffith LG, Swartz MA. Capturing complex 3D tissue physiology in vitro. Nat Rev Mol Cell Biol 2006;7:211–24.

[15] Nelson CM, Bissell MJ. Of extracellular matrix, scaffolds, and signaling: tissue architecture regulates development, homeostasis, and cancer. Annu Rev Cell Dev Biol 2006;22:287–309.

[16] Pastrana E, Silva-Vargas V, Doetsch F. Eyes wide open: a critical review of sphere-formation as an assay for stem cells. Cell Stem Cell.8:486–98.

[17] Sarig R, Baruchi Z, Fuchs O, Nudel U, Yaffe D. Regeneration and transdifferentiation potential of muscle-derived stem cells propagated as myospheres. Stem Cells 2006;24:1769–78.

[18] Li TS, Cheng K, Lee ST, Matsushita S, Davis D, Malliaras K, et al. Cardiospheres recapitulate a niche-like microenvironment rich in stemness and cell-matrix interactions, rationalizing their enhanced functional potency for myocardial repair. Stem Cells 2010;28:2088–98.

[19] Cho HJ, Lee HJ, Chung YJ, Kim JY, Yang HM, Kwon YW, et al. Generation of human secondary cardiospheres as a potent cell processing strategy for cell-based cardiac repair. Biomaterials 2012;34:651–61.

[20] Huang GS, Dai LG, Yen BL, Hsu SH. Spheroid formation of mesenchymal stem cells on chitosan and chitosan-hyaluronan membranes. Biomaterials 2011;32:6929–45.

[21] Cheng NC, Wang S, Young TH. The influence of spheroid formation of human adipose-derived stem cells on chitosan films on stemness and differentiation capabilities. Biomaterials 2012;33:1748–58.

[22] Keller GM. In vitro differentiation of embryonic stem cells. Curr Opin Cell Biol 1995;7:862–9.

[23] Agastin S, Giang UB, Geng Y, Delouise LA, King MR. Continuously perfused microbubble array for 3D tumor spheroid model. Biomicrofluidics 2011;5:24110.

[24] Lin RZ, Chou LF, Chien CC, Chang HY. Dynamic analysis of hepatoma spheroid formation: roles of E-cadherin and beta1-integrin. Cell Tissue Res 2006;324:411–22.

[25] Golebiewska A, Brons NH, Bjerkvig R, Niclou SP. Critical appraisal of the side population assay in stem cell and cancer stem cell research. Cell Stem Cell.8:136–47.

[26] Dalerba P, Clarke MF. Cancer stem cells and tumor metastasis: first steps into uncharted territory. Cell Stem Cell 2007;1:241–2.

[27] Mani SA, Guo W, Liao MJ, Eaton EN, Ayyanan A, Zhou AY, et al. The epithelial-mesenchymal transition generates cells with properties of stem cells. Cell 2008;133:704–15.

[28] Vazin T, Schaffer DV. Engineering strategies to emulate the stem cell niche. Trends Biotechnol 2010;28:117–24.

[29] Brawley C, Matunis E. Regeneration of male germline stem cells by spermatogonial dedifferentiation in vivo. Science 2004;304:1331–4.

[30] Kai T, Spradling A. Differentiating germ cells can revert into functional stem cells in Drosophila melanogaster ovaries. Nature 2004;428:564–9.

[31] Hendrix MJ, Seftor EA, Seftor RE, Kasemeier-Kulesa J, Kulesa PM, Postovit LM. Reprogramming metastatic tumour cells with embryonic microenvironments. Nat Rev Cancer 2007;7:246–55.

[32] Fischbach C, Chen R, Matsumoto T, Schmelzle T, Brugge JS, Polverini PJ, et al. Engineering tumors with 3D scaffolds. Nat Methods 2007;4:855–60.

[33] Danet GH, Pan Y, Luongo JL, Bonnet DA, Simon MC. Expansion of human SCID-repopulating cells under hypoxic conditions. J Clin Invest 2003;112:126–35.

[34] Gustafsson MV, Zheng X, Pereira T, Gradin K, Jin S, Lundkvist J, et al. Hypoxia requires notch signaling to maintain the undifferentiated cell state. Dev Cell 2005;9:617–28.

[35] Morrison SJ, Csete M, Groves AK, Melega W, Wold B, Anderson DJ. Culture in reduced levels of oxygen promotes clonogenic sympathoadrenal differentiation by isolated neural crest stem cells. J Neurosci 2000;20:7370–6.

[36] Covello KL, Kehler J, Yu H, Gordan JD, Arsham AM, Hu CJ, et al. HIF-2alpha regulates Oct-4: effects of hypoxia on stem cell function, embryonic development, and tumor growth. Genes Dev 2006;20:557–70.

[37] Manasek FJ, Burnside MB, Waterman RE. Myocardial cell shape change as a mechanism of embryonic heart looping. Dev Biol 1972;29:349–71.

[38] Ingber D. Extracellular matrix and cell shape: potential control points for inhibition of angiogenesis. J Cell Biochem 1991;47:236–41.

[39] Erickson GR, Gimble JM, Franklin DM, Rice HE, Awad H, Guilak F. Chondrogenic potential of adipose tissue-derived stromal cells in vitro and in vivo. Biochem Biophys Res Commun 2002;290:763–9.

[40] Hoben GM, Koay EJ, Athanasiou KA. Fibrochondrogenesis in two embryonic stem cell lines: effects of differentiation timelines. Stem Cells 2008;26:422–30.

[41] McBeath R, Pirone DM, Nelson CM, Bhadriraju K, Chen CS. Cell shape, cytoskeletal tension, and RhoA regulate stem cell lineage commitment. Dev Cell 2004;6:483–95.

[42] Liu Y, Clem B, Zuba-Surma EK, El-Naggar S, Telang S, Jenson AB, et al. Mouse fibroblasts lacking RB1 function form spheres and undergo reprogramming to a cancer stem cell phenotype. Cell Stem Cell 2009;4:336–47.

[43] Song X, Zhu CH, Doan C, Xie T. Germline stem cells anchored by adherens junctions in the Drosophila ovary niches. Science 2002;296:1855–7.

[44] Jones PH, Harper S, Watt FM. Stem cell patterning and fate in human epidermis. Cell 1995;80:83–93.

[45] Jensen UB, Lowell S, Watt FM. The spatial relationship between stem cells and their progeny in the basal layer of human epidermis: a new view based on whole-mount labelling and lineage analysis. Development 1999;126:2409–18.

[46] Garcion E, Halilagic A, Faissner A, ffrench-Constant C. Generation of an environmental niche for neural stem cell development by the extracellular matrix molecule tenascin C. Development 2004;131:3423–32.

[47] Keung AJ, Kumar S, Schaffer DV. Presentation counts: microenvironmental regulation of stem cells by biophysical and material cues. Annu Rev Cell Dev Biol 2010;26:533–56.

[48] Osafune K, Takasato M, Kispert A, Asashima M, Nishinakamura R. Identification of multipotent progenitors in the embryonic mouse kidney by a novel colony-forming assay. Development 2006;133:151–61.

[49] Huangfu D, Maehr R, Guo W, Eijkelenboom A, Snitow M, Chen AE, et al. Induction of pluripotent stem cells by defined factors is greatly improved by small-molecule compounds. Nat Biotechnol 2008;26:795–7.